

**Aptavalve-gated Mesoporous Carbon Nanospheres image Cellular Mucin and provide
On-demand Targeted Drug Delivery**

*Chengyi Li,¹ Min Qian,¹ Shanshan Wang,¹ Huilin Jiang¹, Yilin Du¹, Jianxin Wang¹, Weiyue Lu¹
Niren Murthy² and Rongqin Huang^{1*}*

¹ Department of pharmaceutics, School of Pharmacy, Key Laboratory of Smart Drug Delivery, Ministry of Education, Fudan University, Shanghai 201203, P. R. China.

² Department of Bioengineering, University of California, Berkeley, California 94720, USA.

E-mail: rquang@fudan.edu.cn

Table of contents in Supporting Information :

1. Experimental Sections

- 2. Table S1.** Linear range and detection limit of the detection of MUC1.
- 3. Table S2.** IC50 of MCF-7 cells under different treatments.
- 4. Figure S1.** SEM images of OMCN and TEM images of OMCN and Dox-OMCN-P₀.
- 5. Figure S2.** Fluorescent quenching effect as a function of OMCN/Dox ration and reaction time.
- 6. Figure S3.** Schematic illustration of P₀ aptamer.
- 7. Figure S4.** SAXS, XAS and Raman spectrum of Dox-OMCN-P₀.
- 8. Figure S5.** BET surface area and pore size distribution of OMCN and Dox-OMCN-P₀.
- 9. Figure S6.** Quantification of P₀ by UV spectrum.
- 10. Figure S7.** Fluorescent spectra of pH responsive release of Dox-OMCN.
- 11. Figure S8.** Time release curve of Dox-OMCN in different pH solutions.
- 12. Figure S9.** Fluorescent spectra of Dox-OMCN capped with P₀ (PBS 5.0).
- 13. Figure S10.** MUC1 responsive release of Dox-OMCN-P₀ (PBS 5.0).
- 14. Figure S11.** Dox release curve under the incubation with different concentration of P₀ and MUC1 as function of different time points in PBS 7.4.
- 15. Figure S12.** Fluorescent spectra of Dox-OMCN capped with P₀ (PBS 7.4).
- 16. Figure S13.** MUC1 responsive release of Dox-OMCN-P₀ (PBS 7.4).
- 17. Figure S14.** Dox release curve under the incubation with different concentration of P₀ and MUC1 as function of different time points in bio-mimic solution (PBS 7.4 with 10% FBS).
- 18. Figure S15.** Fluorescent spectra of Dox-OMCN capped with P₀ (PBS 7.4 with 10% FBS).
- 19. Figure S16.** MUC1 responsive release of Dox-OMCN-P₀ (PBS 7.4 with 10% FBS).
- 20. Figure S17.** Fitted curve of MUC1 responsive fluorescent recovery using Infinite M1000 Pro microplate reader (PBS 5.0).
- 21. Figure S18.** Specificity of Dox-OMCN-P₀ aptavalve.
- 22. Figure S19.** Confocal images of MCF-10A cells incubated with Dox-OMCN-P₀.
- 23. Figure S20.** Flow cytometry experiments of MCF-7 and MCF-10A cells.
- 24. Figure S21.** Competitive binding experiment between P₀ and MUC1.

25. **Figure S22.** Flow cytometry fluorescent analysis of MCF-7 responsive to increased MUC1 and linear equation based on the quantification results of confocal microscopy.
26. **Figure S23.** Cell toxicity of MCF-7 responsive to increased MUC1.
27. **Figure S24.** Cell toxicity of Dox-OMCN-P₀ and Dox.
28. **Figure S25.** Cell toxicity of OMCN-P₀.
29. **Figure S26.** Photothermal effect of Dox-OMCN-P₀ via irradiation of 980 nm infrared radiation.
30. **Figure S27.** Thermal images quantify of tumor-bearing nudes after irritations with 980 nm infrared radiation.
31. **Movie S1.** Real-time thermal video of tumor-bearing nudes treated with saline and Dox-OMCN-P₀ respectively, then irritations with 980 nm infrared radiation.

Experimental Sections

Materials and reagents: Doxorubicin hydrochloride was purchased from Beijing Huafeng-Lianbo technology Co. Ltd. (Beijing, China). P₀ aptamer (5' to 3': GCAGTTGATCCTTTGGATACCCTGG), Cytochrome C and lysozyme were purchased from Shanghai Sangon Biotechnology Co. Ltd. (Shanghai, China). MUC1 (N→C: PDTRPAPGSTAPPAHGVTSAPDTRPAPGSTAPPAHGV TSA) was purchased from China Peptides Co. Ltd. (Shanghai, China). Fetal bovine serum (FBS) was purchased from Biological Industries (USA). Phosphate buffer solution (PBS), Penicillin and Streptomycin were obtained from Hyclone (USA). RPMI 1640 medium, Dulbecco's modified Eagle medium (DMEM), trypsin and l-glutamine were purchased from Gibco (USA). Live/Dead cell viability assay kit was purchased from Thermo fisher Scientific (USA). Cell Counting Kit-8 reagent was purchased from Dojindo Molecular Technologies, Inc. (Japan). Phenol, formaldehyde, triethylamine, Tris and other chemical reagents were purchased from Sinopharm Chemical Reagent Co. Ltd (Shanghai, China).

Apparatus: Scanning electron microscope (SEM) and transmission electron microscopy (TEM) images were obtained by Ultra 55 electron microscope (Zeiss, Germany) and Tecnai G2 F20 S-Twin electron microscope (FEI, USA), respectively. Small Angle X-ray Scattering (SAXS) and X-ray diffraction patterns (XRD) were analyzed through NanoStar U SAXS System (Bruker, Germany) using Cu K α radiation (40 kV, 35 mA) and D8 Advance & Davinci Design diffractometer (Bruker, Germany) using Cu K α radiation at 40 kV and 60 mA, respectively. Raman spectra were observed using a 403 spectrometer (SPEX, France). Hydrated size distribution were measured by Zetasizer Nano ZS (Malvern, UK). BET surfaces area and pore size were conducted using Tristar II 3020 (Micromeritics Instrument Co., USA). Ultraviolet spectra were performed on UV-2401PC (Shimadzu Co., Japan). Fluorescent emission spectra were carried based on a G9800A

fluorescence spectrophotometer (Angilent, USA) and Infinite M1000 Pro microplate reader (Tecan, Switzerland). The confocal microscopy images were gained through LSM710 (Zeiss, Germany). Flow cytometry experiments were performed by FACS Aria II (Becton, Dickinson and Company, USA). Cell toxicity assays were measured by synergy 2 microplate reader (Bio Tek, USA). Live/Dead images were observed under a DMI4000D fluorescent microscope (Leica, Germany). Living imaging was conducted and analyzed by Maestro-2 system (PerkinElmer Company, USA). Thermal experiments were irradiated based on ruby laser (Changchun Leishi, China) and images were taken by VarioCAM HD inspect 600 infrared imager (InfraTec., Germany).

Synthesis of OMCN: Phenol (1.2 g) and formaldehyde solution (4.2 mL, 37 wt%) were gently mixed and stirred in alkaline condition at 70 °C for 30 min, then pellucid Pluronic F127 solution (1.92 g/30 mL H₂O) was added and stirred at 66 °C for 2 h. After that, ultrapure water (100 mL) was added and stirred for another 17 h. Then, aging process was conducted through diluting reaction solution (17.7 mL) with water (56 mL) at 130 °C for 24 h. After that, yellow powders washed with absolute ethyl alcohol and water were freeze-dried. Finally, dry pellets were calcined at above 750°C for 6 h under N₂ atmosphere and MCN was obtained. OMCN was gained through oxidation of MCN using the acid mixture of H₂SO₄/HNO₃ = 3/1 (v/v) through ultrasonication and 4 h stirring at 60 °C.

Dox loading and pH responsive release: Dox was loaded into different concentrations of OMCN through stirring for 9 h in room temperature at dark place, after which fluorescence was observed. Further, time-dependent manner was determined by agitate 400 µg/mL of OMCN with 20 µg/mL of Dox and fluorescence were measured at different time points. After the Dox loading process, Dox-OMCN was dialyzed (PBS, pH = 7.4, 6.0 and 5.0). The dialysis process was that,

reaction solutions containing Dox-OMCN were centrifuged and redispersed in 1 mL PBS, then shake in dialysis bag with 20 mL dialysate. Finally, fluorescence was measured at every time point.

Construction of Dox-OMCN-P₀ aptavalve and MUC1 responsive assay in PBS: P₀ aptamer with different concentrations was added into Dox-OMCN and stirred in room temperature for 1 h. UV spectra of P₀ aptamer were obtained before and after incubation with Dox-OMCN and the concentration of P₀ capped on OMCN was calculated based on the P₀ calibration curve. After dialysis in PBS 5.0, 7.4 and bio-mimic solution (PBS 7.4 with 10% FBS), fluorescence was measured at every time point. For the MUC1 detection, MUC1 with different concentrations (0 - 10.6 μmol/L) was incubated with Dox-OMCN-P₀ for 1 h, after dialysis in PBS 5.0, 7.4 and bio-mimic solution (PBS 7.4 with 10% FBS), fluorescence was measured at every time point. Moreover, MUC1 with lower concentrations (0.1 - 5.3 μmol/L) was also detected using the Infinite M1000 Pro microplate reader the same as fluorescence spectrophotometer. The specificity of cap opening mechanism of Dox-OMCN-P₀ was also investigated by comparing to 20 μmol/L cytochrome C and 20 μmol/L lysozyme. Equation of limit detection was listed below.

$$LD = \frac{3\Delta}{K}$$

(LD: limit of detection; Δ is the standard deviation of ten sequential background signals, which the concentration of MUC1 is zero; k is its corresponding slope of calibration curve for MUC1-responsive fluorescence recovery).

Cell culture and Construction of MCF-7 tumor-bearing nude mice models: MCF-7 and MCF-10A cells were cultured in RPMI 1640 medium (15% FBS) and DMEM (10% FBS) supplemented with penicillin (100 U/mL), streptomycin (100 μg/mL) and l-glutamine (2 mmol/L) at 37 °C and in a humidified atmosphere containing 5% CO₂, respectively.

All animal procedures were approved by the animal ethics committee of Fudan University. Balb/c nude mice (female, 5 weeks old) were purchased from Bikai animal Co. Ltd., and housed under

standard conditions. MCF-7 cells (2×10^6) were slowly subcutaneously injected into the right flank of mice. After 3 weeks, nude mice models were prepared for the animal experiments.

Confocal microscopy and flow cytometry: Dox-OMCN-P₀ (60 µg/mL of OMCN) was incubated with MCF-7 and MCF-10A cells for 4 h, 8 h and 12 h, respectively, then confocal microscopy images were obtained by Confocal Laser Scanning Microscopy (CLSM). For P₀ aptamer competitive binding assays, 100-fold excessive P₀ aptamer (3 µmol/L) were preincubated with MCF-7 cells for 12 h, then Dox-OMCN-P₀ (60 µg/mL of OMCN) was added and images were taken by CLSM at 4 h, 8 h and 12 h, respectively. The cells without incubation of Dox-OMCN-P₀ were used as controls. For the quantitative experiments of cytomembrane MUC1, MUC1 with increased concentrations (1.06 µmol/L – 10.6 µmol/L) and Dox-OMCN-P₀ (60 µg/mL of OMCN) were added into MCF-7 cells, and images were captured at 10 h by CLSM and Flow cytometry. The mean fluorescence intensity was measured by Zen software (black edition) and BD FACSDiva (6.1.3 version), then fit linear equation was calculated. The concentration of MUC1 existed in cytomembrane was defined as the absolute value of point intersection between linear equation and X-axis. For the comparison of Dox-OMCN-P₀ intake and Dox release between MCF-7 and MCF-10A cells using flow cytometry assay, cells were trypsin-treated and analyzed via FlowJo software after incubated with Dox-OMCN-P₀ (60 µg/mL of OMCN) for 12 h.

Live/Dead and cytotoxicity assay: MCF-7 cells were incubated with Dox-OMCN-P₀ (15 - 1000 µg/mL of OMCN) for 24 h, then images were gained after treatment with Live/Dead cell viability assay kit for 20 min. For cytotoxicity assays, MCF-7 cells were incubated with Dox-OMCN-P₀ (15 - 1000 µg/mL of OMCN) and free Dox (0.75 - 50 µg/mL) for 24 h and 36 h, respectively. Then the cytotoxicity was performed using Cell Counting Kit-8 reagent. MCF-7 cells without any treatments and MCF-10A cells incubated with Dox-OMCN-P₀ (15 - 1000 µg/mL of OMCN) for 24 h were

used as controls. MUC1 responsive cell toxicity was conducted through incubated MCF-7 cells with Dox-OMCN-P₀ (60 µg/mL of OMCN) for 10 h, then cell toxicity were measured. Besides, material toxicity was investigated with different concentrations of OMCN-P₀ (15 - 1000 µg/mL of OMCN) for 24 h.

Living imaging: MCF-7 tumor-bearing and normal nude mice were separately injected with 100 µL Dox solution (i.v, 100 µg/mL) and 100 µL Dox-OMCN-P₀ solution (i.v, 1 mg/mL of OMCN), and observed before and after injection for 2 h, 4 h, 8 h and 12 h, respectively, by Maestro-2 system. Then, tumor and main organs (heart, liver, spleen, lung and kidney) were separated and imaged. And the quantification of florescence intensity was conducted by IVIS software.

Fluorescent analysis of tissue homogenate: MCF-7 tumor-bearing and normal nude mice were separately injected with 100 µL Dox-OMCN-P₀ solution (i.v, 1 mg/mL of OMCN), 100 µL Dox solution (i.v, 100 µg/mL), and 100 µL Saline for 8 h, then tumor-bearing nudes were sacrificed and organs were fetched. The process of homogenate (homogenization buffer: 0.3 mol/L HCl with 60% ethyl alcohol) was conducted and the fluorescence was measured.

Thermal experiments: Dox-OMCN-P₀ with different concentrations (30, 60, 120 and 180 µg/mL) and saline were irradiated by a 980 nm laser (1 W/cm²), and then temperatures were recorded at each time point. For *in vivo* thermal effect, MCF-7 tumor-bearing nude mice were irradiated for 5 min (980 nm, 0.5 W/cm²) after intratumorly injected with 100 µL Dox-OMCN-P₀ (0.5 mg/mL) and saline, then temperature changes were recorded by VarioCAM HD inspect 600 infrared imager.

Table S1. Linear range and detection limit of fluorescence spectrophotometer and Infinite M1000 Pro microplate reader for the MUC1 detection.

Medium	Common fluorescence spectrophotometer		Microplate reader Infinite M1000 Pro (Tecan)	
	Linear range	Detection limit	Linear range	Detection limit
PBS	1.06 – 10.6 μ M	101 nM	0.10 – 5.3 μ M	17.5 nM

Table S2. IC₅₀ (μ g/mL) in MCF-7 cells under different treatments.

Drug	Treatment time	
	24 h	36 h
Dox-OMCN-P₀ (μ g/mL)	419.4 (20.97*)	323.6 (16.18*)
Pure Dox (μ g/mL)	11.1	6.58

*Conversed loading amount of Dox.

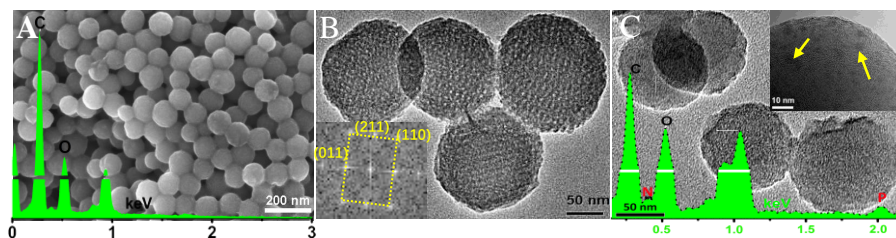


Figure S1. (A) SEM images of OMCN, the inset of which was corresponding elemental analysis. (B) TEM images of OMCN, the inset of which was the corresponding Fourier Transform (FT) pattern. (C) TEM images of Dox-OMCN-P₀, in which the top inset was the high resolution TEM and the bottom inset was the elemental analysis.

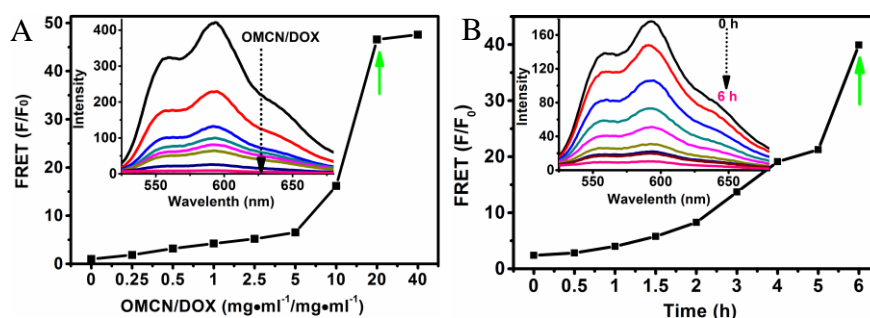


Figure S2. (A) Fluorescence quenching ability of different OMCN/Dox ratios, the inset of which was corresponding fluorescent spectra. (B) Fluorescent quenching effect and corresponding fluorescent spectra of Dox-OMCN as a function of time.

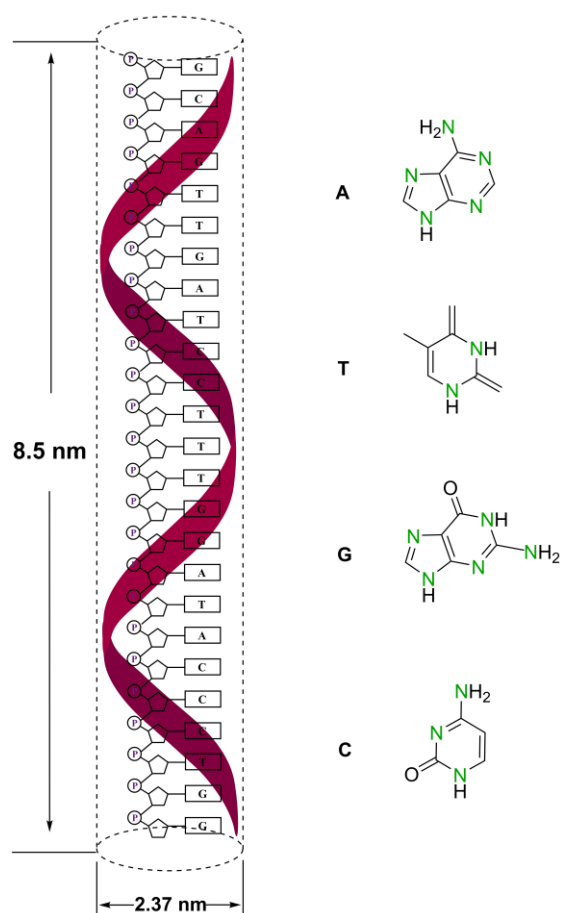


Figure S3. Schematic illustration of the 3-dimensional structure of P₀ aptamer.

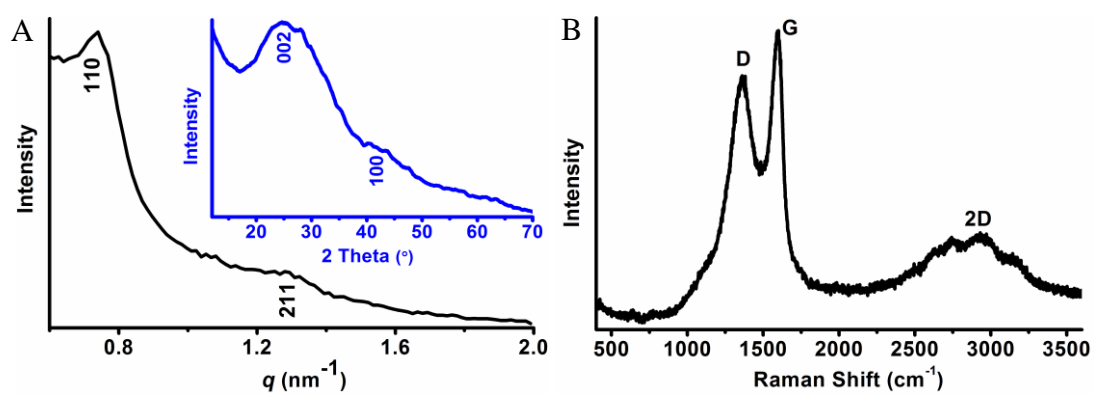


Figure S4. (A) SAXS pattern and corresponding high angle XRD pattern (inset) of Dox-OMCN-P₀. (B) The Raman spectrum of Dox-OMCN-P₀.

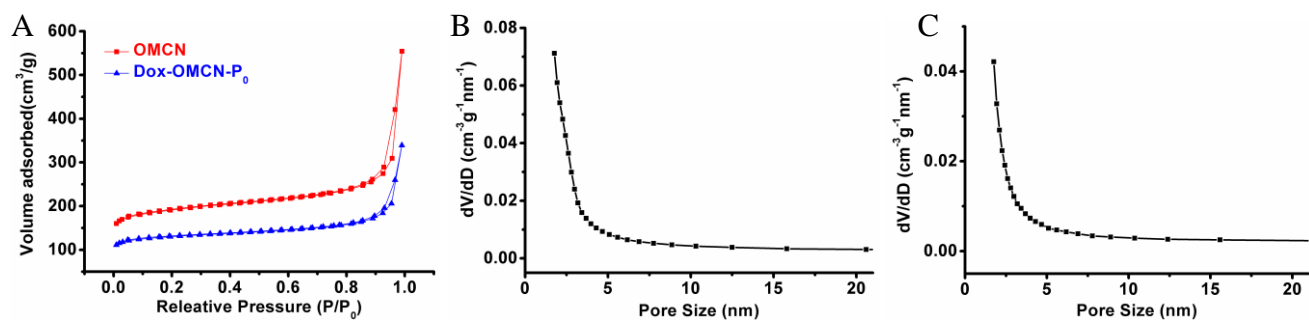


Figure S5. (A) BET nitrogen adsorption and desorption of OMCN and Dox-OMCN-P₀. (B) BJH pore size distribution of OMCN. (C) BJH pore size distribution of Dox-OMCN-P₀.

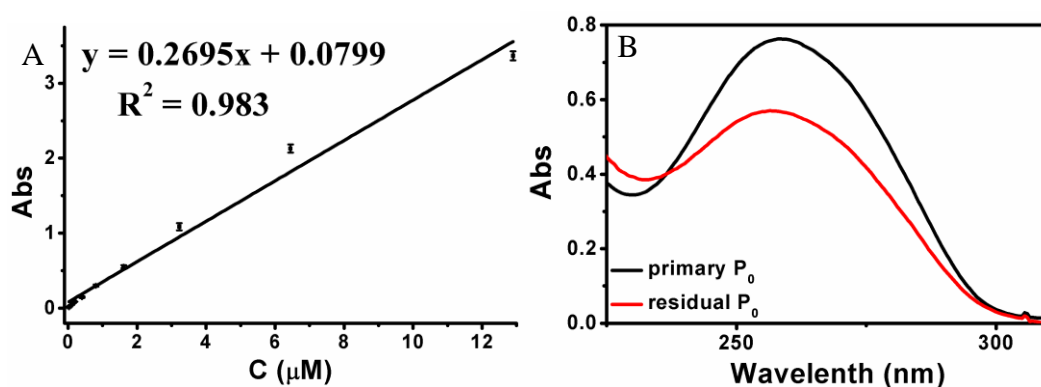


Figure S6. (A) The calibration UV absorbance curve of P₀ aptamer. Data are represented as mean \pm SD (n = 3). (B) UV spectra of primary P₀ and residual P₀ after incubation with Dox-OMCN. The amount of P₀ absorbed in OMCN was 1.79 μ mol P₀/mg OMCN according to the calibration curve.

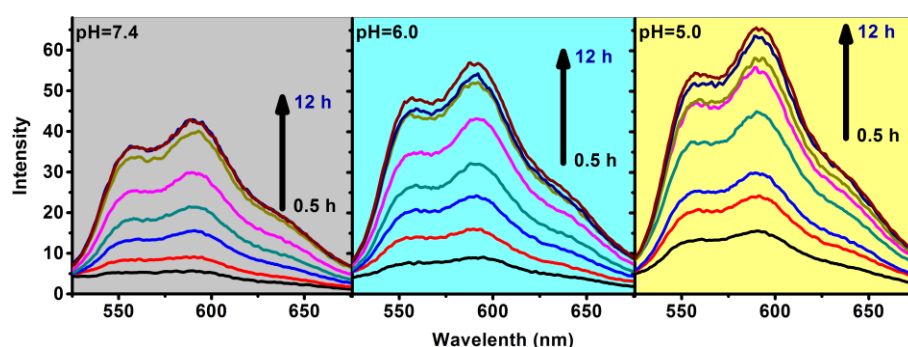


Figure S7. Fluorescent spectra of Dox release along with time in buffer solutions with different pH (pH = 7.4, 6.0 and 5.0).

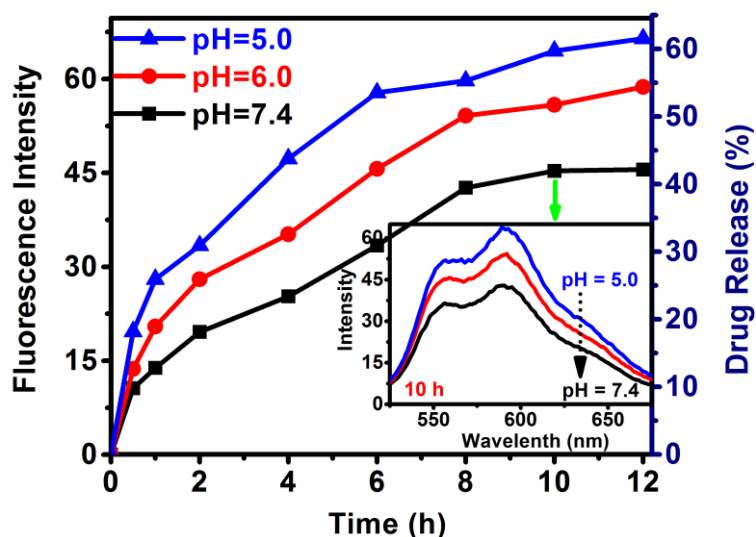


Figure S8. The drug release profiles of Dox-OMCN in PBS (pH = 7.4, 6.0 and 5.0) as a function of time. The inset was the fluorescent spectra of Dox-OMCN in each buffer after 10 h release.

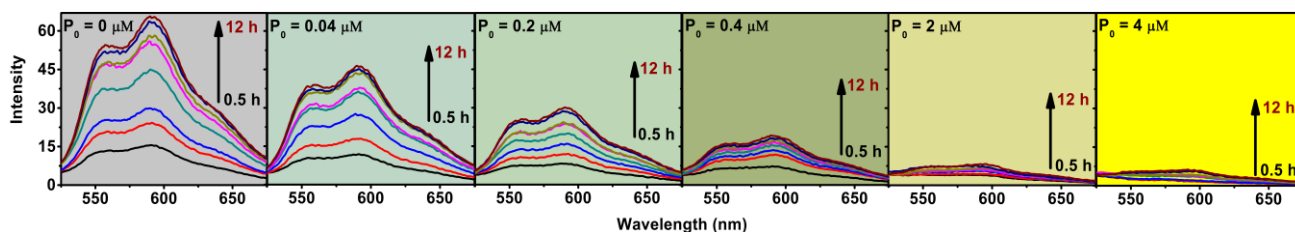


Figure S9. Fluorescent spectra of Dox-OMCN along with time in the presence of P_0 with different concentrations in PBS 5.0.

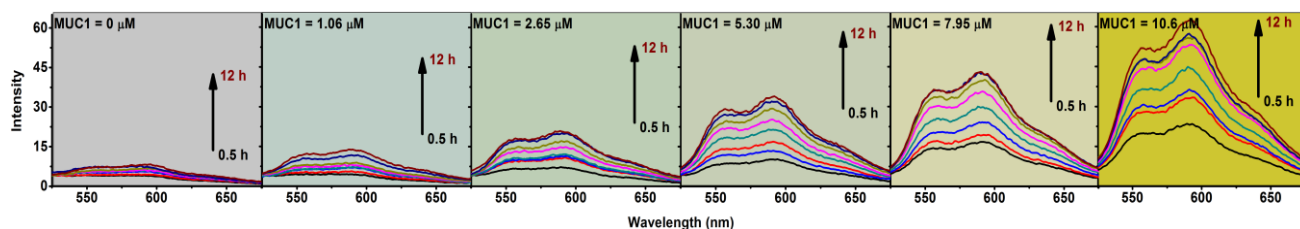


Figure S10. Fluorescent spectra of Dox-OMCN- P_0 along with time in the presence of MUC1 with different concentrations in PBS 5.0.

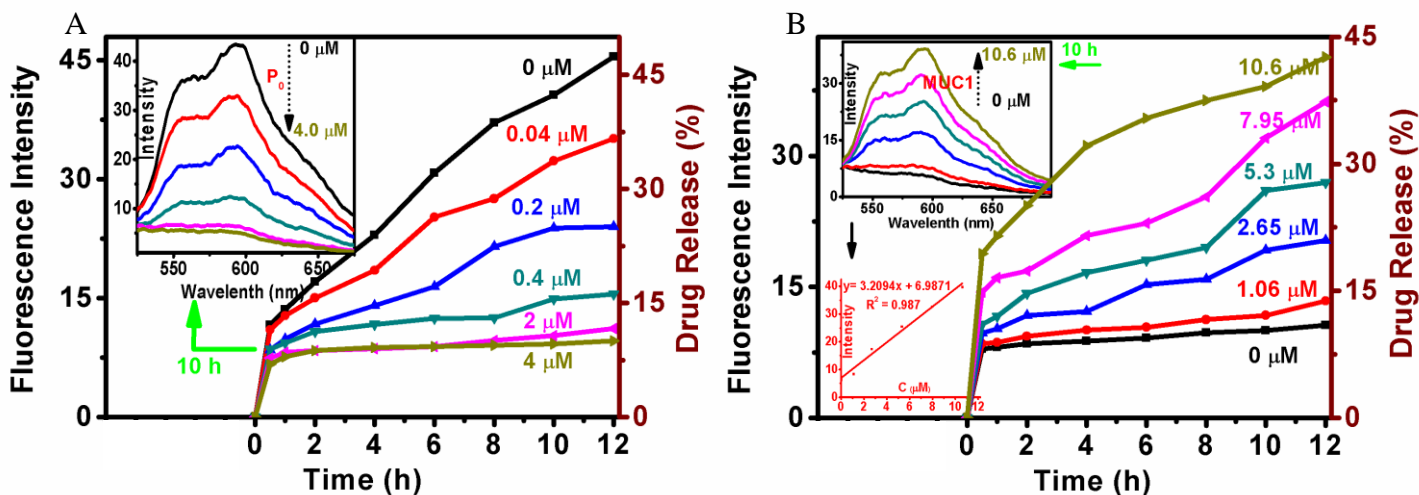


Figure S11. (A) Drug release profiles of Dox-OMCN- P_0 in PBS 7.4 with different concentrations of P_0 cap. The inset was the fluorescent spectra at 10 h release. (B) Drug release profiles of Dox-OMCN- P_0 in PBS 7.4 with different MUC1 concentrations. The insets were the fluorescent spectra and the linear curve between MUC1 concentrations and Dox fluorescence intensities after 10 h release.

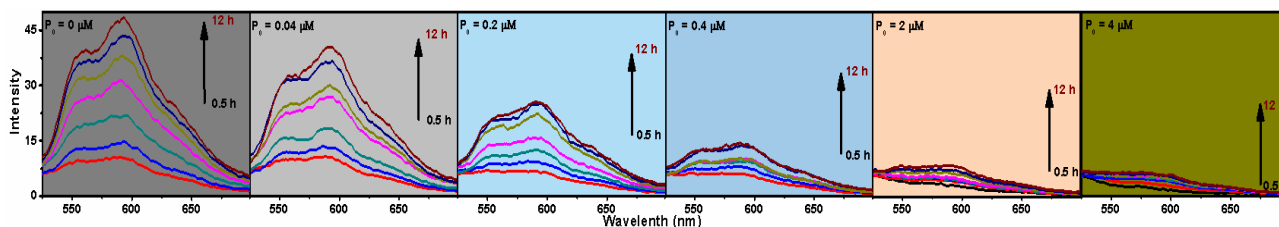


Figure S12. Fluorescent spectra of Dox-OMCN along with time in the presence of P_0 with different concentrations in PBS 7.4.

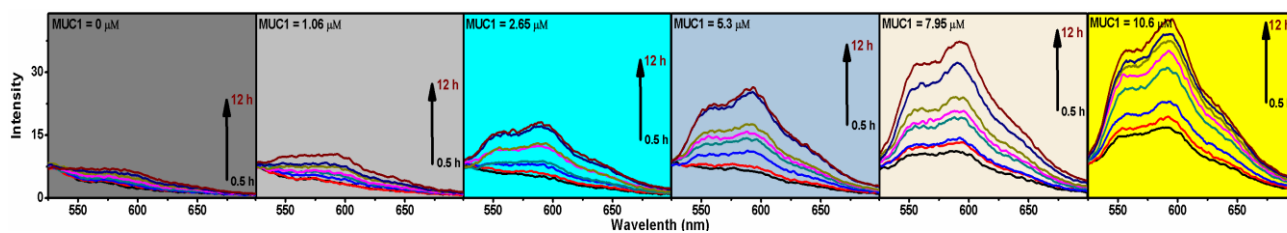


Figure S13. Fluorescent spectra of Dox-OMCN- P_0 along with time in the presence of MUC1 with different concentrations in PBS 7.4.

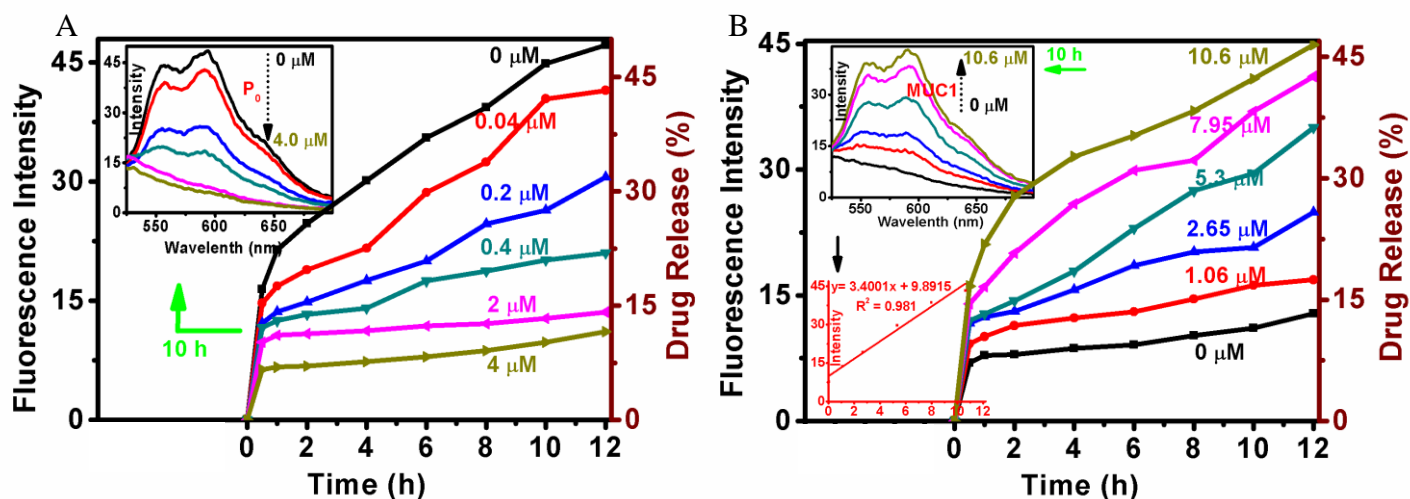


Figure S14. (A) Drug release profiles of Dox-OMCN- P_0 in bio-mimic solution (PBS 7.4 with 10% FBS) with different concentrations of P_0 cap. The inset was the fluorescent spectra at 10 h release. (B) Drug release profiles of Dox-OMCN- P_0 in bio-mimic solution (PBS 7.4 with 10% FBS) with different MUC1 concentrations. The insets were the fluorescent spectra and the linear curve between MUC1 concentrations and Dox fluorescence intensities after 10 h release.

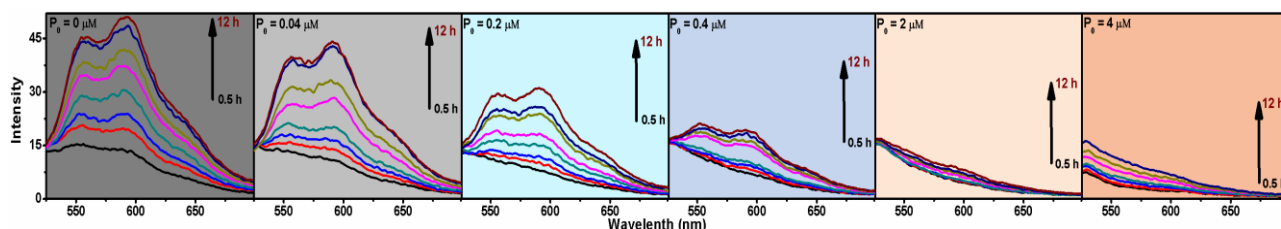


Figure S15. Fluorescent spectra of Dox-OMCN along with time in the presence of P_0 with different concentrations in bio-mimic solution (PBS 7.4 with 10% FBS).

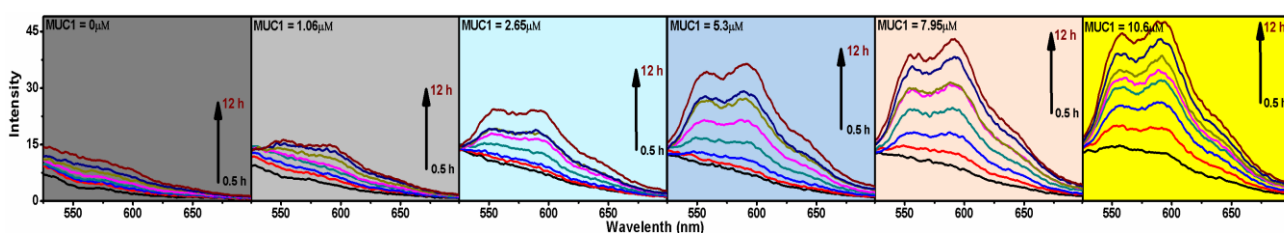


Figure S16. Fluorescent spectra of Dox-OMCN- P_0 along with time in the presence of MUC1 with different concentrations bio-mimic solution (PBS 7.4 with 10% FBS).

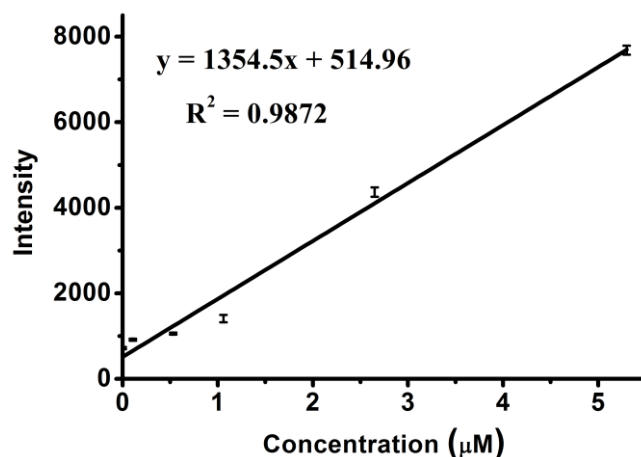


Figure S17. The calibration curve for MUC1-responsive fluorescence recovery/drug release using the Infinite M1000 Pro microplate reader (PBS 5.0). Data are represented as mean \pm SD (n = 3).

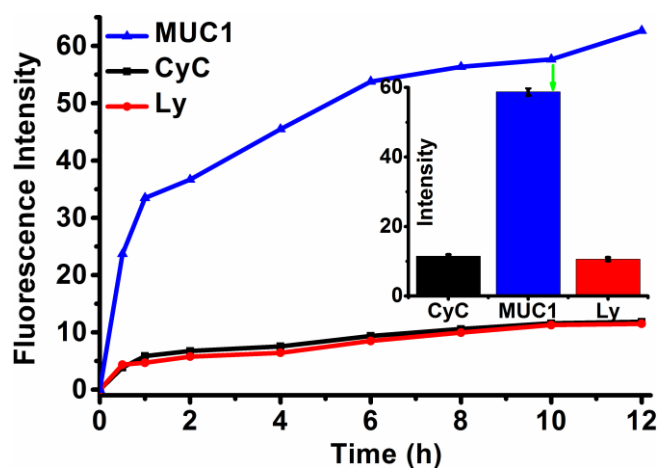


Figure S18. The fluorescent intensity of Dox-OMCN-P₀ in the presence of cytochrome C (CyC, 20 μmol/L), MUC1 (10.6 μmol/L) or lysozyme (Ly, 20 μmol/L) under different incubation time. The inset was the histogram of fluorescent intensity after 10 h incubation. Data are represented as mean \pm SD (n = 3).

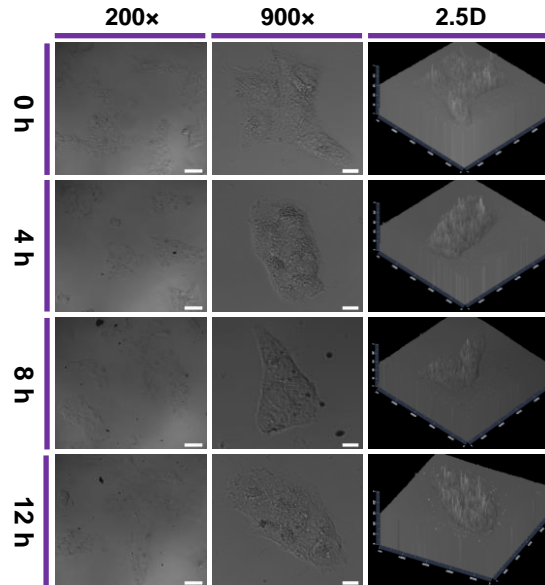


Figure S19. Different magnified confocal fluorescence microscopy images and corresponding 2.5 dimensional sectional views of MCF-10A cells incubated with Dox-OMCN- P_0 for different time periods. Scale bar: 50 μm (200 \times), 10 μm (900 \times).

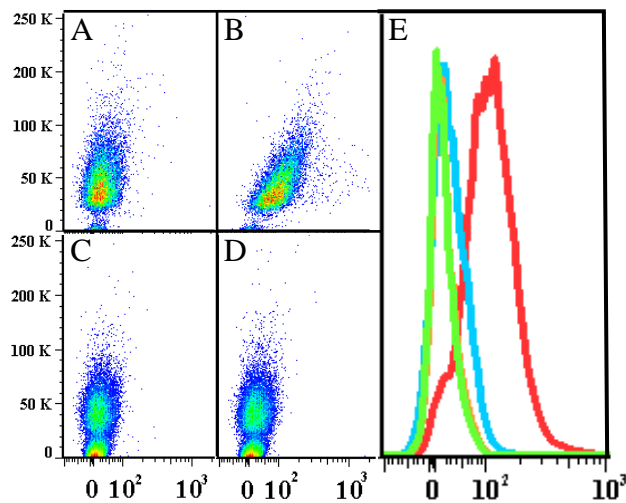


Figure S20. (A-D) Flow cytometry scatter diagrams of MCF-7 cancer cells (A, B) and MCF-10A normal cells (C, D) incubated without (A, C) or with Dox-OMCN- P_0 (B, D), respectively. (E) Flow cytometry curves of MCF-7 cancer cells (Red, Blue) and MCF-10A normal cells (Green, Orange) incubated without (Blue, Orange) or with Dox-OMCN- P_0 (Red, Green), respectively.

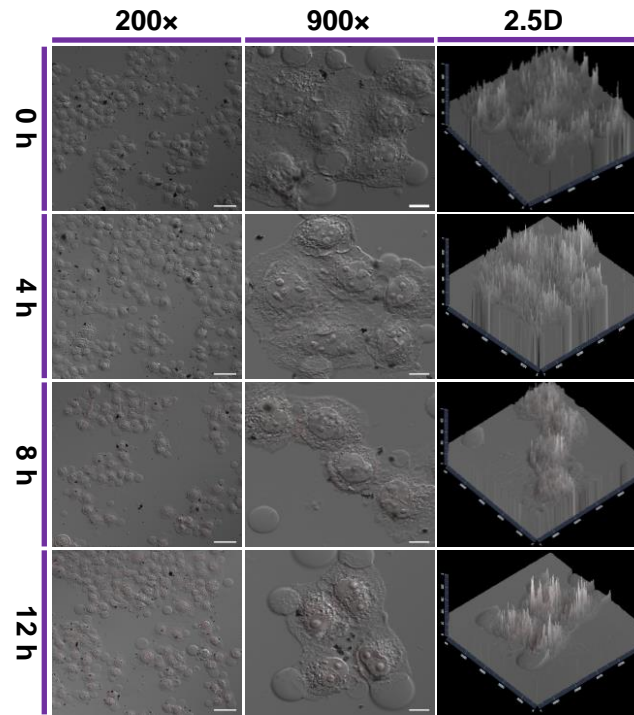


Figure S21. Different magnified confocal fluorescence microscopy images and corresponding 2.5 dimensional sectional views of MCF-7 cells pre-incubated with P₀ (30 $\mu\text{mol/L}$) for 12 h and then incubated with Dox-OMCN-P₀ for different time periods. Scale bar: 50 μm (200 \times), 10 μm (900 \times).

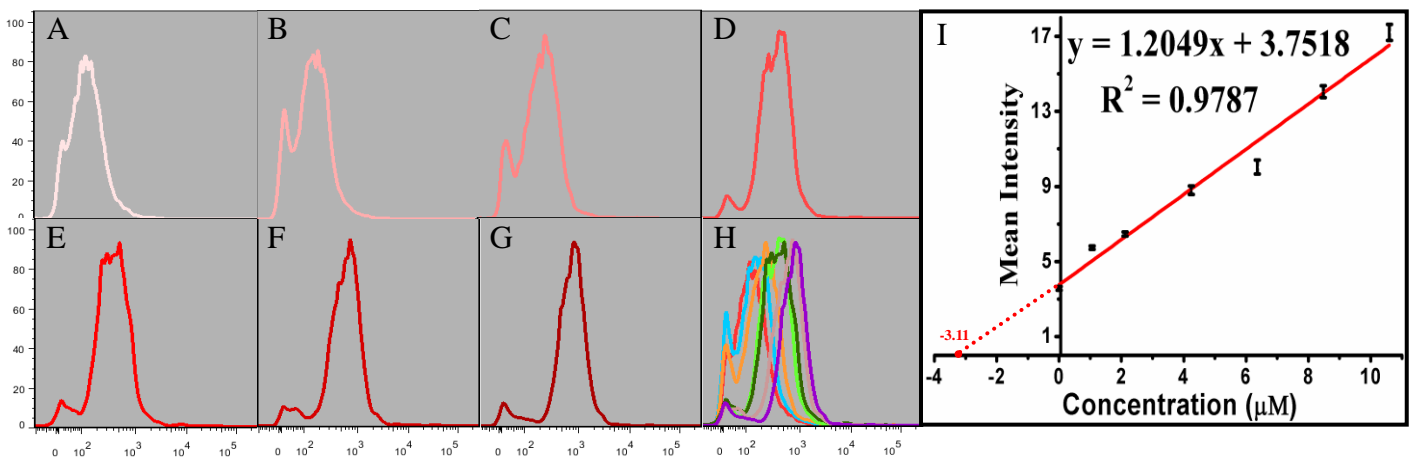


Figure S22. (A-G) Flow cytometry analysis of MCF-7 cells incubated with Dox-OMCN-P₀ for 10 h after pre-adding different concentrations of MUC1 (A-G: 0-10.6 $\mu\text{mol/L}$). (H) Merge results of A-G. (I) Linear curve of the standard addition method for MUC1 detection based on the quantification of confocal fluorescence microscopy images. Data are represented as mean \pm SD (n = 3).

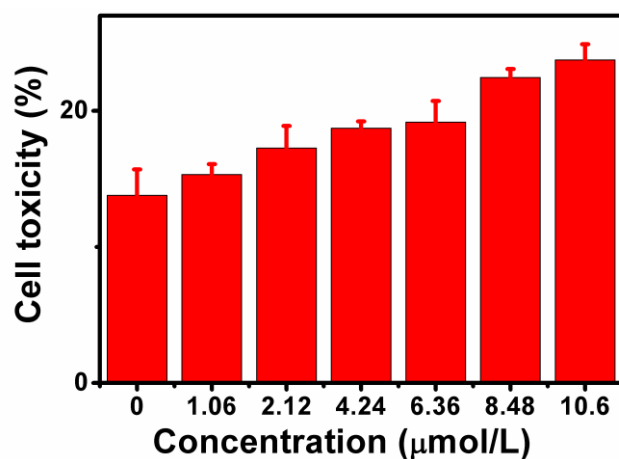


Figure S23. Cell toxicity of MCF-7 cells after incubation with Dox-OMCN-P₀ and different concentrations of MUC1 for 24 h. Data are represented as mean \pm SD (n = 3).

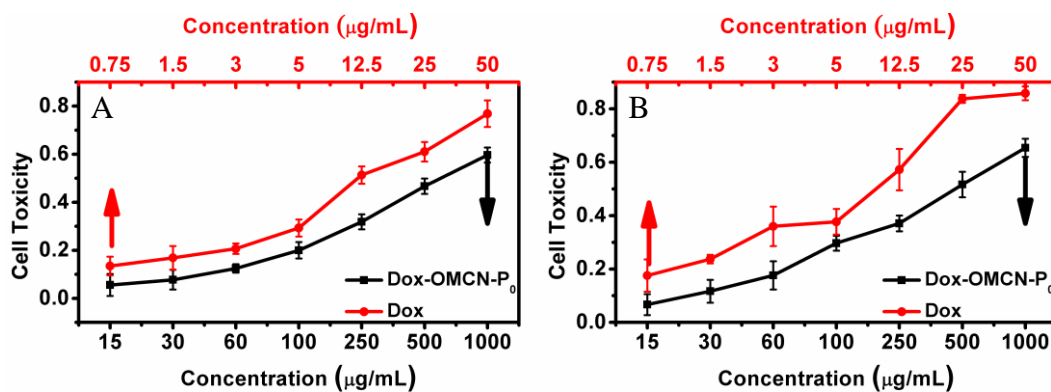


Figure S24. Cell toxicity of MCF-7 cells after incubation with Dox-OMCN-P₀ and pure Dox of the same drug concentration for 24 h (A) and 36 h (B), respectively. Data are represented as mean \pm SD (n = 3).

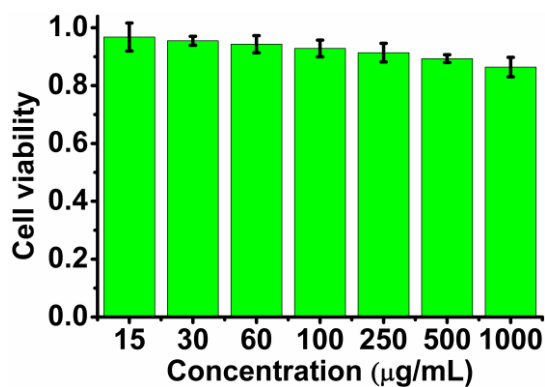


Figure S25. Cytotoxicity of MCF-7 cells after 24 h incubation of OMCN-P₀. Data are represented as mean \pm SD (n = 3).

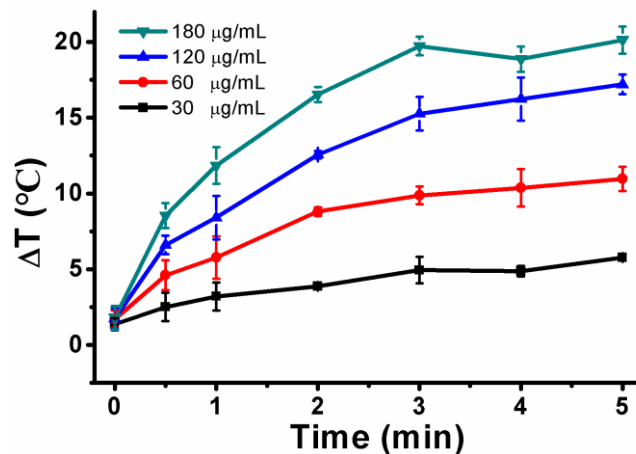


Figure S26. The photothermal heating temperature changes (ΔT) between Dox-OMCN- P_0 solutions with different concentrations and water via NIR irradiation (1 W/cm^2 , 980 nm) for different time periods. Data are represented as mean \pm SD ($n = 3$).

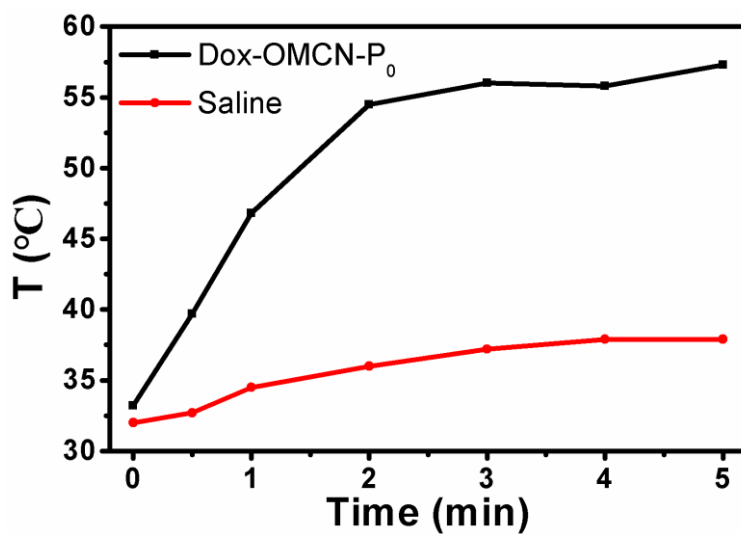


Figure S27. Temperature variations of tumor sites injected with Dox-OMCN- P_0 and saline, respectively, via 980 nm NIR laser irradiation (0.5 W/cm^2) for different time periods.

Movie

Movie S1. The movie of the 980 nm NIR photothermal therapy (0.5 W/cm^2 , 5 min) of tumors in mice after injection with Dox-OMCN- P_0 and saline, respectively.